International Journal of Rotating Machinery
1997, Vol. 3, No. 3, pp. 179–187
Reprints available directly from the publisher
Photocopying permitted by license only

Advanced Compressor Loss Correlations, Part II: Experimental Verifications

M. T. SCHOBEIRI*

Turbomachinery Performance Laboratory, Texas A&M University, CS., TX 77843-3123

(Received 2 August 1996)

Reliable efficiency calculation of high-subsonic and transonic compressor stages requires a detailed and accurate prediction of the flow field within these stages. Despite the tremendous progress in turbomachinery computational fluid mechanics, the compressor designer still uses different loss correlations to estimate the total pressure losses and thus the efficiency of the compressor stage. The new shock loss model and the modified diffusion factor, developed in Part I, were implemented into a loss calculation procedure. In this part, correlations for total pressure loss, profile loss, and secondary loss coefficients are presented, using the available experimental data. Based on the profile loss coefficients, correlations were also established for boundary layer momentum thickness. These correlations allow the compressor designer to accurately estimate the blade losses and therefore the stage efficiency.

Keywords: Compressor, transonic, subsonic, loss, correlations

INTRODUCTION

The theoretical background and discussion presented in Part I of this paper showed a direct correlation between the profile losses and the boundary layer quantities, particularly the boundary layer momentum thickness. Investigations by NACA, summarized in NASA SP-36 [1976] and briefly reviewed in Part I, showed that measuring the total pressure losses can experimentally determine the momentum thickness. Further investigations by Gostelow and Krabacher [1967], Gostelow [1971], Seylor and Smith [1967], Seylor and Gostelow [1968], Gostelo et al. [1968], Krabacher and Gostelow [1976a,b], and Monsarrat et al. [1969] deal with the spanwise distribution of the total pressure and the total pressure loss coefficient. For the aerodynamic design of a single stage compressor, Monsarrat et al. [1969] presented correlations between the profile loss parameter and the diffusion factor using the experimental data by Sulam et al. [1970]. The loss correlations by Monsarrat et al. [1969] are frequently used as a guideline for designing compressor stages with the profile similar to that described by Monsarrat et al. [1969]. Gostelow et al. [1968] performed systematic and detailed experimental investigations on four different rotors to determine

*Corresponding author. Tel.: (409) 845-0819

the optimum blade camber line shape. Although the experimental data revealed certain systematic tendencies, no attempt was made to develop a correlation to describe the loss situation in a systematic manner. These facts gave impetus to consider the above experimental data in the present analysis.

ANALYSIS OF EXPERIMENTAL DATA

To establish the loss correlations, the existing available experimental data were reevaluated, particularly those in Gostelow et al. [1968] and Krabacher and Gostelow [1976a,b], which used four single stage compressors with multi-circular-arc profiles. A detailed description of the compressor facility and the stages are found in their reports. The data analysis used the following information: (1) the total pressure losses as a function of diffusion factor in the spanwise direction, (2) inlet, exit, and incidence angles, (3) Mach numbers, (4) velocities, and (5) geometry. To consider the compressibility effect discussed in Part I of this paper, the modified diffusion factor D_m was obtained using the information from Gostellow's report mentioned previously. Regression analysis was used for a systematic evaluation of the loss parameters. Figures (1a) to (1d) show the results. Starting from an immersion ratio $H_r = (R_t - R)/(R_t - R_h) = 10\%$, Fig. (1a) shows the loss parameter as a function of a modified diffusion factor for the investigated rotors 1B, 2B, and 2D in the reports by Gostelow and Krabacher [1967], Gostelow [1971], Seylor and Smith [1967], Seylor and Gostelo [1968], Gostelo et al. [1968], Krabacher and Gostelow [1976a,b]. For the sake of clarity, all the measured data are shown uniformly with filled squares. As shown in Fig (1a) and in all subsequent figures, a systematic dependency is clearly visible and the individual rotors do not exhibit any deviatory characteristics. The introduction of the modified diffusion factor with compressibility effect has caused a shift of D_m to higher values. Figures (1b) to (1d) exhibit a similar dependency for $H_r = 50$, 70 and 90%, where the smallest losses are encountered at $H_r = 60$–70. Moving further toward the hub at $H_r = 90\%$, the total pressure losses experience a continuous increase attributed to higher friction losses and the secondary flow caused by the secondary vortices at the hub. A comparison of the loss parameters plotted in Figs. (1a)–(1d) shows that the total pressure losses in the tip region ($H_r = 10\%$) are much higher than those in the hub region ($H_r = 90\%$). The higher losses at the tip are due to the existing shock losses and the secondary flow effect due to the tip clearance vortices.

CORRELATIONS FOR TOTAL LOSSES, PROFILE LOSSES AND REST LOSSES

Correlations are derived for total loss coefficients, profile loss coefficients, and secondary flow loss coefficients from the available experimental data, particularly those discussed previously. These correlations express the direct dependency of the above losses as a function of modified diffusion factor defined in Part I. Furthermore, correlations for momentum thickness and the diffusion factors are given from the profile loss parameter. To obtain a correlation for the profile loss coefficient (see definition in Part I, Section 2), the shock loss coefficients are calculated and subtracted from the total loss coefficients. By definition, this so called profile loss coefficient not only includes the primary losses (see definition in Part I) but also contains the losses due to the secondary flow. As pointed out in Part I, the secondary flow losses assume higher values by approaching the hub/tip regions, respectively. The profile losses correspond to primary losses only at the design section, which includes only the total losses due to the profile friction. Figure (2) shows the total pressure loss parameter as a function of modified diffusion factor with the immersion ratio as a parameter. The highest loss parameter is encountered near the tip. The losses continuously decrease by moving toward the blade midsection up to $H_r = 0.6$. The total pressure loss coefficient assumes a minimum at $H_r = 0.7$. At this radius, the secondary flow effect apparently disappears completely, so that the total pressure loss coef-

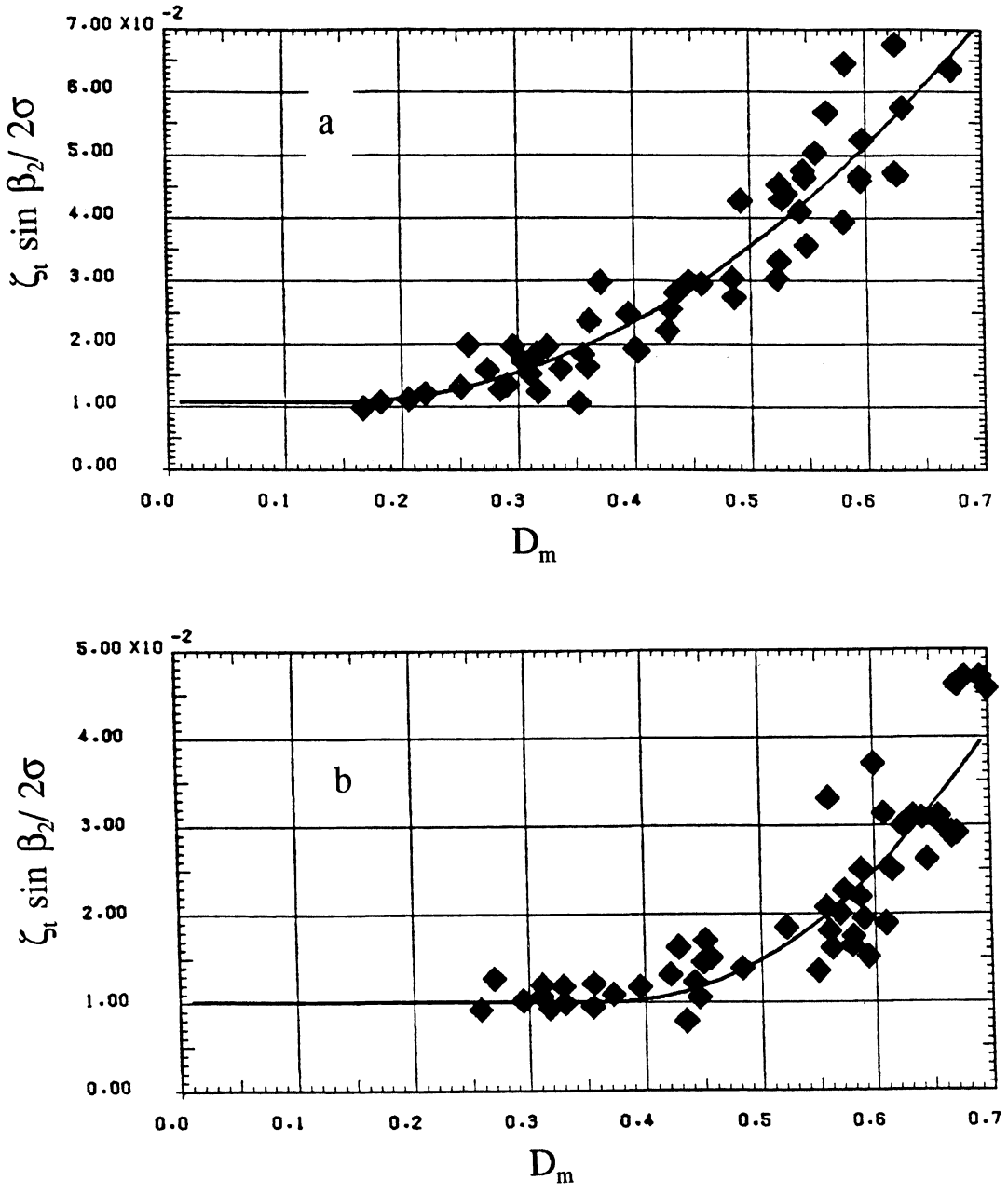

FIGURE 1 a, b Total pressure loss parameter as a function of modified diffusion factor with immersion ratio H_r as parameter for (a) H_r = 10% and (b) H_r = 50% from the tip. Experiments from *NASA-CR-45481-45485*, rotors: 1B, 2B, 2D.

ficient corresponds to the primary loss coefficient. For immersion ratios greater than H_r = 0.7, the losses start increasing again, which indicates the strong effect of the secondary flow. As previously mentioned, subtracting the shock loss coefficients from the total loss coefficients obtains profile loss coefficients. The resulting profile loss coefficients plotted in Fig. (3) are approximately 30% smaller than the total pressure

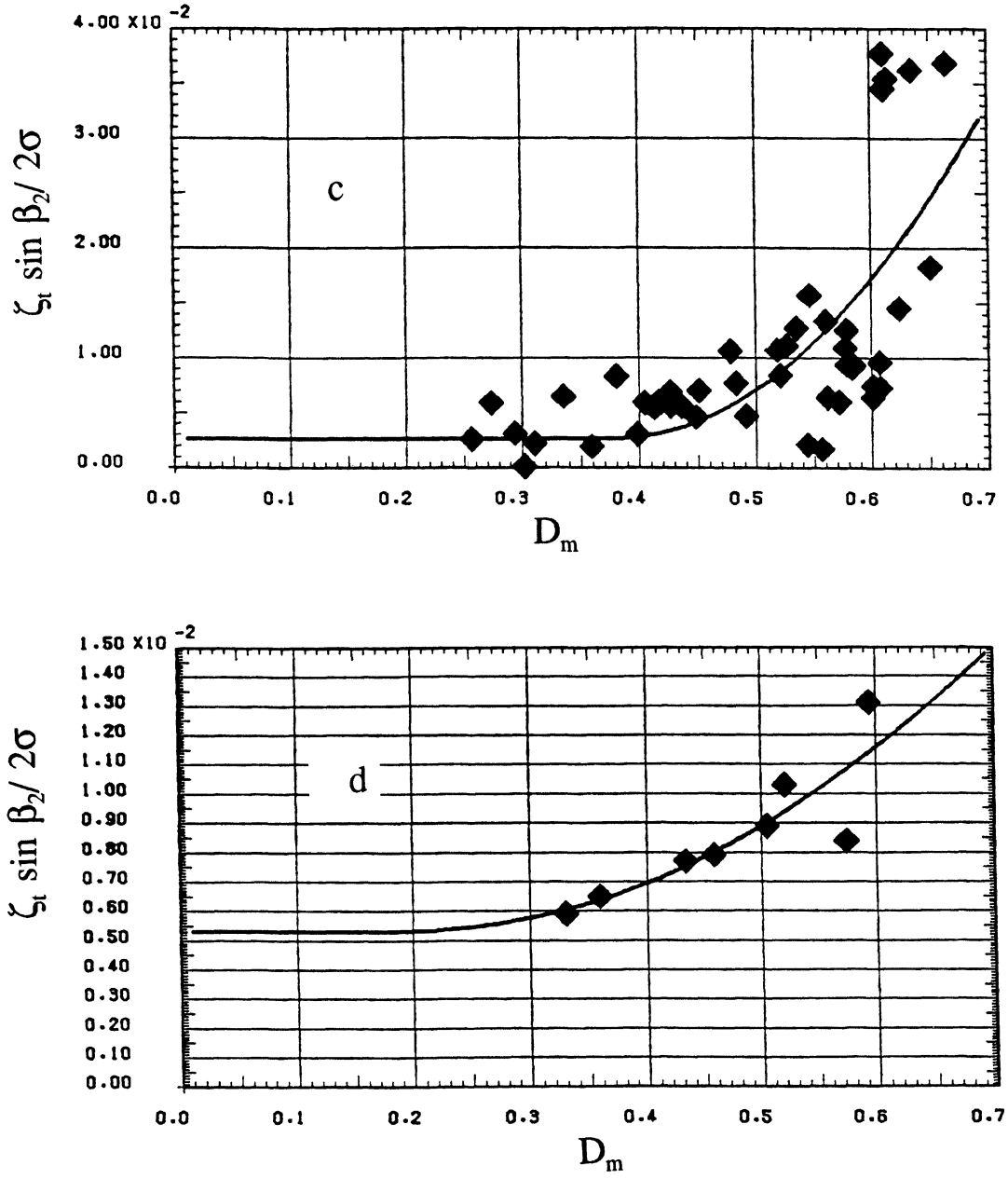

FIGURE 1 c, d Total pressure loss parameter as a function of modified diffusion factor with immersion ratio H_r as parameter for (c) H_r = 70% and (d) H_r = 90%, from the tip. Experiments from *NASA-CR-45481-45485*, rotors: 1B, 2B, 2D.

loss coefficient shown in Fig. (2). The fact that the total pressure loss coefficients exhibit a minimum at $H_r = 0.7$, where the secondary flow effect diminishes, enables the compressor designer to estimate the rest losses. To determine the distribution of the rest losses, we start from the profile loss distributions at different spanwise locations and subtract the losses at $H_r = 0.7$. As a result, these rest losses include the

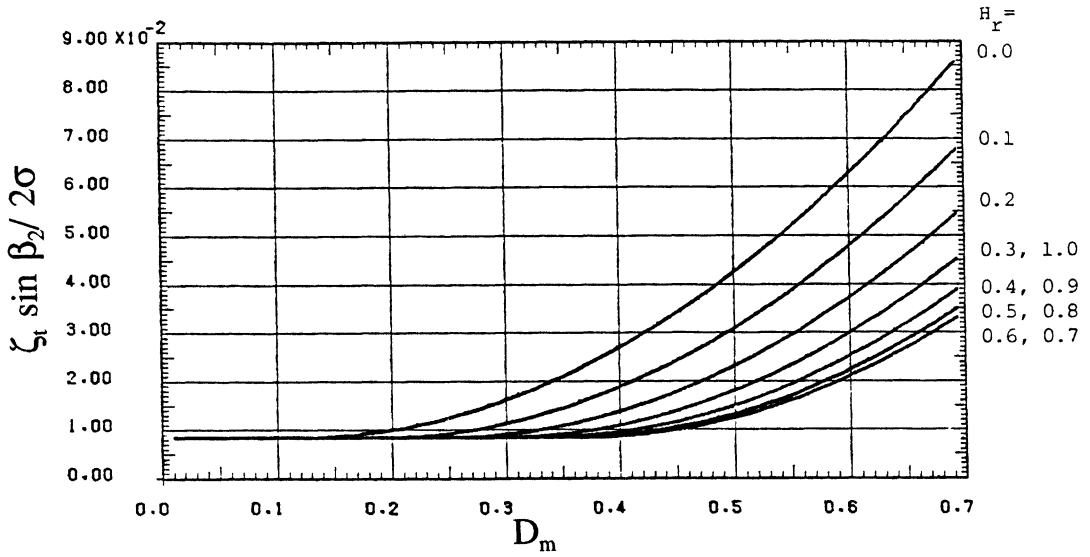

FIGURE 2 Correlations for total pressure loss parameter as a function of modified diffusion factor with the immersion ratio H_r as parameter.

effect of the secondary flows associated with wall boundary layer development and clearance vortices. Figure (4) shows the distribution of the rest loss parameter as a function of the modified diffusion factor. Figure (4) exhibits a linear dependency of the rest loss parameter as a function of the modified diffusion factor with the immersion ratio as a parameter. Since the diffusion factor is directly related to the lift force and thus to the lift coefficient ($C_L c/s$) as a linear function, one may conclude that the rest losses are lin-

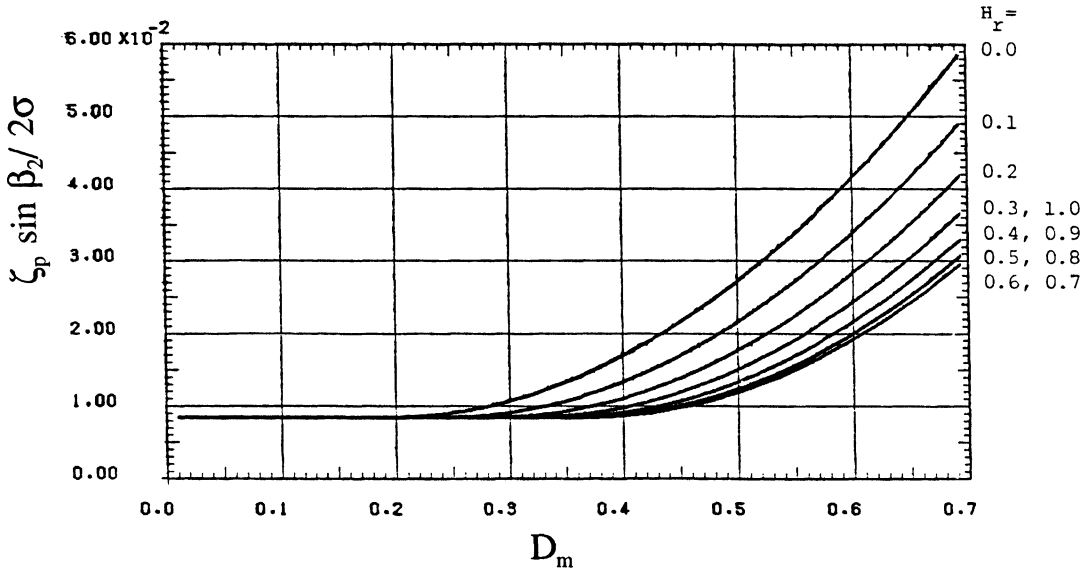

FIGURE 3 Correlations for profile loss parameter as a function of modified diffusion factor with the immersion ratio H_r as parameter.

early proportional to $(C_L c/s)$. This is in agreement with the measurements by Grieb et al. [1975] and in contrast to the correlation proposed earlier by Carter [1948] that includes the term $(C_L c/s)^2$ and is adopted by many other researchers.

CORRELATIONS FOR BOUNDARY LAYER MOMENTUM THICKNESS

As shown in Part I, the profile loss coefficient and the boundary layer momentum thickness are interrelated by:

$$\zeta_p = \sigma \left(\frac{\theta}{c}\right) \left(\frac{\sin\beta_1}{\sin\beta_2}\right)^2 F(H_{12}, H_{32}, \theta, \sigma, c) \qquad (1)$$

The momentum thickness in Eq. (1) is the projection of the suction surface and pressure surface momentum thicknesses given by:

$$\theta \sin\beta_2 \equiv \theta_{SP} = \theta_S + \theta_P \qquad (2)$$

where the subscripts S and P refer to the suction and pressure surface, respectively, and the function F is given by:

$$F = \frac{1 + H_{32}}{\left(1 - \frac{\delta_2}{c}\sigma H_{12}\right)^3} \qquad (3)$$

with H_{12}, H_{32} as the displacement and energy form factors, θ as the boundary layer momentum thickness, σ as the solidity, and c as the blade chord. In the literature (see also Hirsch [1978] and Swan [1961]), the function F is frequently approximated as a constant with the value $F = 2$. For a realistic velocity distribution, Schobeiri [1987] showed that the value of F may differ from 2. To arrive at a better estimation for F, the boundary layer velocity profile is approximated by several simple functions such as a linear function, a power law, a sine function, and an exponential function. A close examination of the results and their comparison with the experiments showed that the velocity approximation by a power function yields better results. However, the exponential approximation would be more appropriate for those profiles that are close to separation. Using the law function approximation, we arrive at:

$$H_{32} = \frac{H_{12} + 1}{3H_{12} - 1} \qquad (4)$$

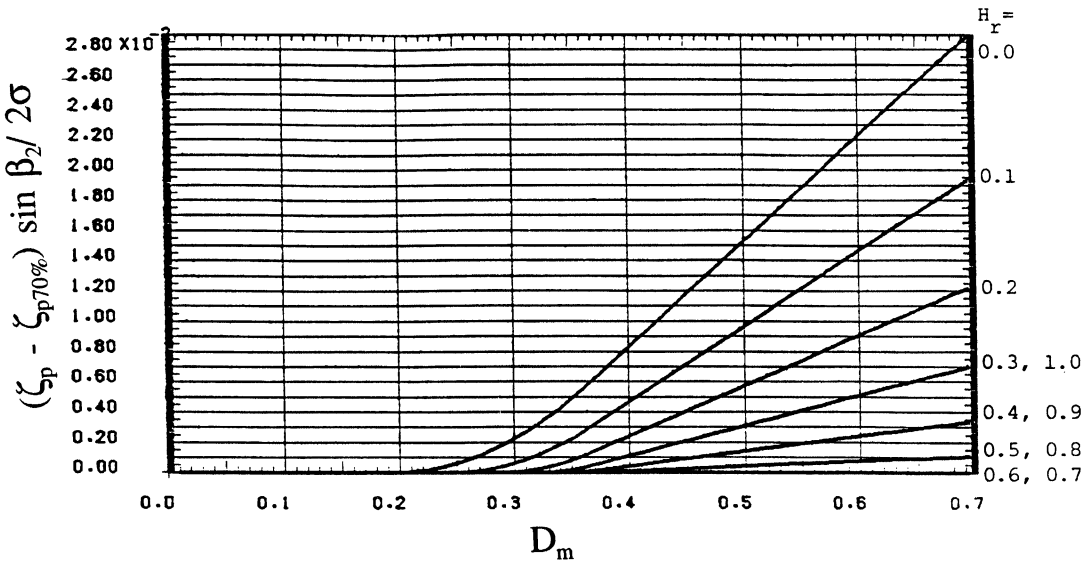

FIGURE 4 Correlations for rest loss parameter as a function of modified diffusion factor with the immersion ratio H_r as parameter.

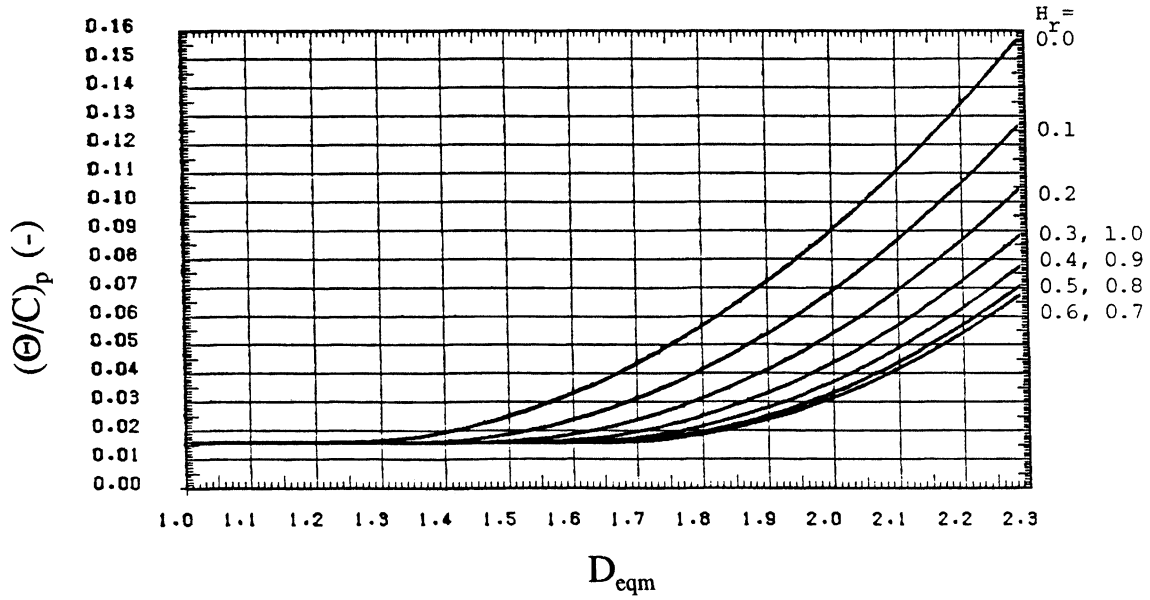

FIGURE 5 Correlations for dimensionless boundary layer momentum thickness as a function of modified diffusion factor with the immersion ratio H_r as parameter.

Introducing Eq. (4) into Eq. (3) and the results into Eq. (1) leads to:

$$\zeta_P = \sigma \left(\frac{\delta_2}{c}\right) \left(\frac{\sin\beta_1}{\sin\beta_2}\right)^2 \left[\frac{\dfrac{4H_{12}}{3H_{12}-1}}{\left(1-\dfrac{\delta_2}{c}\sigma H_{12}\right)^3}\right] \tag{5}$$

With Eq. (5) and (3), the momentum thickness is determined from:

$$\frac{\theta}{c} = \frac{\zeta_p \sin\beta_2}{\sigma} \left(\frac{\sin\beta_2}{\sin\beta_1}\right)^2 \frac{1}{F} \tag{6}$$

Using the profile losses as previously discussed, the correlation for the momentum thickness as a function of modified equivalent diffusion factor (see Part I) are plotted in Fig. (5) with the immersion ratio as a parameter. The highest value for the momentum thickness is encountered in the vicinity of the tip that includes the viscosity effects as well as the secondary flow effects. Similar to the profile losses, the momentum thickness continuously decreases by moving toward the blade midsection up to $H_r = 0.6$. It assumes a minimum at $H_r = 0.7$. At this radius, the secondary flow effect apparently diminishes completely, so that the momentum thickness corresponds to the one generated by the blade surface friction only. For immersion ratios greater that $H_r = 0.7$, the momentum thickness starts increasing again, which indicates the strong effect of the secondary flow.

INFLUENCE OF DIFFERENT PARAMETERS ON PROFILE LOSSES

The correlations presented above are based on experimental results performed on typical high performance compressors with specific flow characteristics and blade geometries similar to those discussed previously. These correlations may be applied to other compressors with similar geometries but different flow conditions by considering the effect of the following individual parameters.

MACH NUMBER EFFECT

Estimating the Mach number effect requires calculating the critical Mach number. When the Mach num-

ber reaches unity locally in a compressor cascade, the corresponding inlet Mach number is said to have reached its critical value. Jansen and Moffat [1967] made the assumptions that below the critical Mach number, the total pressure losses and the turning angle are essentially constant. The pressure losses increase rapidly beyond this value. Using the gas dynamics relations, Jansen and Moffat [1967] determined the local critical Mach number by the following implicit relation:

$$\left(\frac{V_{\max}}{V_1}\right)^2 - 1 = \frac{1 - \left(\frac{2}{k+1} + \frac{k-1}{k+1} M_{1cr}^2\right)^{\frac{k}{(k-1)}}}{-1 + \left(1 + \frac{k-1}{2} M_{1cr}^2\right)^{\frac{k}{(k-1)}}} \tag{7}$$

To estimate the critical Mach number directly, Davis [1971] suggested the following explicit relation:

$$M_{1cr} = 2.925 - 2.948\left(\frac{V_{\max}}{V_1}\right) + 1.17\left(\frac{V_{\max}}{V_1}\right)^2 - 0.1614\left(\frac{V_{\max}}{V_1}\right)^3 \tag{8}$$

As seen in Part I, the velocity ratio $V_{\max}/V_1$ is directly related to the circulation function and thus the diffusion factor. With the critical Mach number from Eq. (7) or (8), the profile loss coefficient can be corrected as:

$$\zeta_{pcor} = \zeta_p\,[A(M_1 - M_{1cr}) + 1.0] \tag{9}$$

with $A = 1.8$–2.0 (see Moffat [1967] and Davis [1971]). For DCA-profiles, Dettmering and Grahl [1971] found that Eq. (9) underestimates the correction and suggested the following modified approximation:

$$\zeta_{pcor} = \zeta_p\,\{14.0\left[M_1 - (M_{1cr} - 0.4)^3\right] + 1.0\} \tag{10}$$

REYNOLDS NUMBER EFFECT

This effect is only at lower Reynolds number ranges of practical significance. For high performance compressors, the Reynolds number is high enough so that its changes do not affect the profile losses. The following profile loss correction is suggested for Reynolds number ranges $\mathrm{Re} < 2.5 \times 10^5$:

$$\zeta_{pcor} = \zeta_p \left(\frac{Re}{Re_{cor}}\right)^{0.2} \tag{11}$$

BLADE THICKNESS EFFECT

To consider the effect of the thickness ratio t/c, the boundary layer momentum thickness may be corrected using the correlation by Fottner [1979].

$$\left(\frac{\theta}{c}\right)_{cor} = \frac{\theta}{c}\left(6.6\,\frac{t}{c} + 0.34\right) \tag{12}$$

CONCLUSION

In the second part of this paper, correlations were established for the total pressure loss coefficient, profile loss coefficients, and the secondary loss coefficients. Based on the profile loss coefficients, correlations were also established for boundary layer momentum thickness. The modified diffusion factor, discussed in Part I, was a major variable of the correlations with the immersion ratio as the parameter. Different loss parameters as well as boundary layer momentum thickness can be calculated for the compressor stages with similar blade profiles using the stage velocity diagram. These correlations allow the compressor designer to accurately estimate the blade losses and therefore the stage efficiency. Some corrections are recommended for inlet flow conditions different from those for which the above correlations were established.

NOMENCLATURE

c	blade chord length
D_{eqm}	modified equivalent diffusion factor
D_m	modified diffusion factor (see part I)

F	auxiliary function
H_{12}	form factor, $H_{12} = \delta/\theta$
H_r	immersion ratio
M	Mach number
Re	Reynolds number
S	spacing
t	Thickness
V	velocity
α, β	flow angles
ζ	loss coefficient
η	velocity ratio
Θ	boundary layer momentum thickness, shock expansion angle
σ	cascade solidity $\sigma = c/s$

SUB- AND SUPERSCRIPTS

a, t	axial, tangential
cr	critical
max	maximum
P, S	pressure, suction surface
C, S, R	Cascade, stator, rotor

References

Carter, A. D. S., (1948) Three-Dimensional flow theories for axial compressors and turbines, *Proceedings of the Institution of Mechanical Engineers*, Vol. 159, p. 255.

Davis, W. R., (1971) A computer program for the analysis and design of turbomachinery, *Carleton University Report No. ME/A*.

Dettmering, W. and Grahl, K., (1971) Machzahleinfluß auf Verdichtercharakteristik, ZFW 19. Fottner, L., (1979) Answer to questionnaire on compressor loss and deviation angle correlations, AGARD- PEP, 1979. Working Group 12.

Gostelow, J. P., Krabacher, K. W. and Smith, L. H., (1968) Performance comparisons of the high Mach number compressor rotor blading, *NASA CR-1256*.

Gostelow, J. P., (1971) Design performance evaluation of four transonic compressor rotors ASME Transactions, *Journal for Engineering for Power*, Vol. 93, No. 1, pp. 33-41.

Grieb, H., Schill, G. and Gumucio, R., (1975) A semi-empirical method for the determination of multistage axial compressor efficiency. *ASME-Paper 75-GT-11*.

Hirsch, Ch., (1978) Axial compressor performance prediction, survey of deviation and loss correlations *AGARD PEP Working Group* 12.

Gostelow, J. P. and Krabacher, K. W., (1967) Single stage experimental evaluation of high Mach number compressor rotor blading, Part III: Performance of rotor 2E. *NASA CR-54583*.

Jansen, W. and Moffat, W. C. (1967) The off-design analysis of axial flow compressors ASME, *Journal of Eng for Power*, pp. 453–462.

Krabacher, K. W. and Gostelow, J. P., (1967). Single stage experimental evaluation of high Mach number compressor rotor blading, Part IV: Performance of rotor 2D. *NASA CR-54584*.

Krabacher, K. W. and Gostelow, J. P., (1967) Single stage experimental evaluation of high Mach number compressor rotor blading, Part V: Performance of rotor 2B. *NASA CR-54585*.

Monsarrat, N. T., Keenan, M. J. and Tramm, P. C., (1969). Design report: Single stage evaluation of high Mach number compressor stages, *NASA CR-72562 PWA-3546*.

NASA SP-36 NASA Report 1976.

Schobeiri, M. T., (19787) Verlustkorrelationen für transsonische Kompressoren, *BBC-Studie*, TN-87/20, 1987.

Seylor, D. R. and Smith, L. H., (1967) Single stage experimental evaluation of high Mach number compressor rotor blading, Part I: Design of rotor blading. *NASA CR-54581*, *GE R66fpd321P*.

Seylor, D. R. and Gostelow, J. P., (1967) Single stage experimental evaluation of high Mach number compressor rotor blading, Part II: Performance of rotor 1B, *NASA CR-54582*, *GE R67fpd236*.

Sulam, D. H., Keenan, M. J. and Flynn, J. T., (1970) Single stage evaluation of highly loaded high Mach number compressor stages. II Data and performance of a multi-circular arc rotor. NASA CR-72694 PWA-3772.

Swan, W. C., (1961) A practical method of predicting transonic compressor performance, *ASME Journal for Engineering and Power*, Vol. 83, pp. 322–330.

MANEY
publishing

The Institute of Materials, Minerals & Mining

ENERGY MATERIALS

NEW FOR 2006

Materials Science & Engineering for Energy Systems

Maney Publishing on behalf of the Institute of Materials, Minerals and Mining

Economic and environmental factors are creating ever greater pressures for the efficient generation, transmission and use of energy. Materials developments are crucial to progress in all these areas: to innovation in design; to extending lifetime and maintenance intervals; and to successful operation in more demanding environments. Drawing together the broad community with interests in these areas, *Energy Materials* addresses materials needs in future energy generation, transmission, utilisation, conservation and storage. The journal covers thermal generation and gas turbines; renewable power (wind, wave, tidal, hydro, solar and geothermal); fuel cells (low and high temperature); materials issues relevant to biomass and biotechnology; nuclear power generation (fission and fusion); hydrogen generation and storage in the context of the 'hydrogen economy'; and the transmission and storage of the energy produced.

As well as publishing high-quality peer-reviewed research, *Energy Materials* promotes discussion of issues common to all sectors, through commissioned reviews and commentaries. The journal includes coverage of energy economics and policy, and broader social issues, since the political and legislative context influence research and investment decisions.

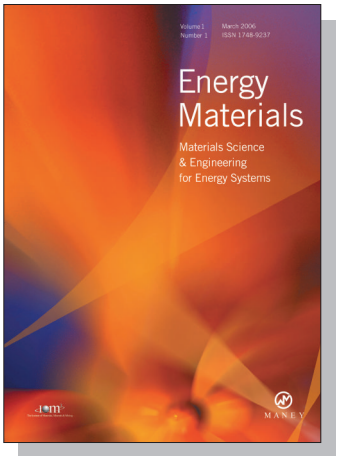

CALL FOR PAPERS

Contributions to the journal should be submitted online at **http://ema.edmgr.com**

To view the Notes for Contributors please visit: **www.maney.co.uk/journals/notes/ema**

Upon publication in 2006, this journal will be available via the Ingenta Connect journals service. To view free sample content online visit: **www.ingentaconnect.com/content/maney**

SUBSCRIPTION INFORMATION

Volume 1 (2006), 4 issues per year
Print ISSN: 1748-9237 Online ISSN: 1748-9245
Individual rate: £76.00/US$141.00
Institutional rate: £235.00/US$435.00
Online-only institutional rate: £199.00/US$367.00
For special IOM^3 member rates please email **subscriptions@maney.co.uk**

For further information please contact:
Maney Publishing UK
Tel: +44 (0)113 249 7481 Fax: +44 (0)113 248 6983 Email: subscriptions@maney.co.uk
or
Maney Publishing North America
Tel (toll free): 866 297 5154 Fax: 617 354 6875 Email: maney@maneyusa.com

For further information or to subscribe online please visit
www.maney.co.uk